Using Planetary Occultations of Radio Sources for Frame-Tie Measurements Part I: Motivation and Search for Events

R. P. Linfield
Tracking Systems and Applications Section

When a planet passes in front of a compact extragalactic radio source as seen from a radio telescope on Earth, timing measurements of the occultation can establish a radio-planetary frame-tie. Two of the three frame-tie parameters can be derived from a single occultation. Twenty-two occultation events in the period 1988–2000 have been found for the planets Mercury–Jupiter. Some of these events involve sources that are too weak or are too large to provide useful frame-tie measurements. However, seven events have good potential to yield frame-tie measurements in the 5–100 nanoradian range, improving on the current 150-nanoradian determination. The first event, an occultation by Venus in July 1988, has been successfully observed.

I. Introduction

The technique of Very Long Baseline Interferometry (VLBI) allows highly accurate navigation of planetary spacecraft [1]. The position of a spacecraft on the sky can be measured to an accuracy of 5–50 nanoradians (nrad) with respect to the radio reference frame by conventional VLBI observations, with 1–2 nrad possible in a local reference frame [2]. The radio frame is defined by several hundred compact extragalactic radio sources [3], whose positions are known to 5–10 nrad from VLBI observations. These radio sources are at distances of 10^8 parsecs (3×10^{21} km) or greater and are believed to be very massive. It is therefore thought that their relative motions are much less than 1 nrad over timescales of decades (e.g., 1000 km/sec transverse velocity at 10^8 parsecs gives a 0.01 nrad/yr angular velocity). Time variations in the offset between the emission centroid and the center of mass of the object will be much larger, on the order of 1 nrad [4]. The internal consistency of the radio frame will be a factor of $\sim \sqrt{N}$ smaller, where N is the number of sources used to define the frame.

For most planetary missions, target-relative navigation is needed. For example, knowledge of the position of a spacecraft with respect to Titan or Jupiter is more important than knowledge of its position with respect to the radio frame. This leads to the concept of the planetary reference frame, defined by the positions of the Sun, the planets, and their satellites (relative to the solar system barycenter) as a function of time [5]. The current positional accuracies of this frame, as seen from Earth, are approximately 150 nrad for Mercury, 50 nrad for

Venus, 25 nrad for Mars, 500 nrad for Jupiter and Saturn, 1000 nrad for Uranus and Neptune, and 5000 nrad for Pluto [5].

The offset between the radio and planetary reference frames can be expressed as three Euler angles. For the most accurately known orbits (those of Mars and Earth), these Euler angles are known to 50–150 nrad (the largest value is for the offset in right ascension) [6]. These Euler angles constitute the radio-planetary frame-tie. Over a period of years, the tie between the radio frame and a specific set of planetary ephemerides changes because the current system of ephemerides is not truly inertial [7]. The position error of a planet in the radio frame is the sum of the error of the orbit of that planet in the planetary frame (i.e., the ephemeris error) and the frame-tie error. The total position error is substantially larger than a typical VLBI position measurement error for every planet. Therefore, the value of VLBI measurements applied to target-relative tracking is limited in most cases by how accurately the positions of the planets are known in the radio frame. (Possible exceptions exist for missions to Jupiter and Saturn. A series of very accurate position measurements in the radio frame during approach is sensitive to the spacecraft–planet separation through measurements of the spacecraft's acceleration [8].)

Improving the frame-tie knowledge is difficult, as the radio emission from planets is too diffuse for VLBI observations, and the positions of sources in the radio frame cannot be measured by the techniques used to determine planetary orbits (e.g., radar ranging and spacecraft encounters).

This article describes one method for performing frame-tie measurements: planetary occultations of compact radio sources. The expected rate of occurrence of such events is calculated, and an upper limit to the accuracy is derived. The search for events is described, and the current set of known events is presented.

II. Planetary Occultations

There are two techniques that directly measure the position of a planet in the radio frame (i.e., they measure the sum of the frame-tie error and the ephemeris error). The first is imaging of the thermal emission of a planet or one of its natural satellites with the Very Large Array (VLA) [6]. Because it is difficult to determine the center of mass from a radio image, this technique is limited to objects of small angular size in the outer solar system: Uranus, Neptune, Titan, and the Galilean satellites. The second technique involves planetary occultations of compact radio sources. These occultations occur when the path of a planet on the sky crosses the position of a radio source. By observing the disappearance of the radio source behind the planet (ingress) and its later reemergence (egress), the position of the planet at the epoch of the occultation can be determined relative to that of the radio source, and ultimately with respect to the radio frame. As is shown below, this technique is primarily useful for the planets Mercury, Venus, Mars, and Jupiter, with possible use for Saturn. The power received from the radio source and planet as a function of time is known as the occultation light curve.

For two reasons, useful measurements of planetary positions require that the radio source that is occulted be compact (much less than 1 arcsec in angular size). The first reason is that VLBI observations of the radio source are needed to accurately determine its position in the radio frame. Only compact radio sources can be detected with VLBI; accurate VLBI position measurements require sources < 10 nrad in extent. The second reason concerns the occultation itself. The light curve is the convolution of the light curve from a point source with the brightness distribution of the actual source; features in the light curve corresponding to angular structure smaller than the source size are washed out.

The path of a planet on the sky follows the ecliptic within a few degrees, with ecliptic latitude usually varying much more slowly than ecliptic longitude. A typical occultation geometry is shown in Fig. 1. The midpoint of the occultation (the mean of the epoch of ingress and egress) is the time when the planet and the compact radio source have the same position along the direction of motion of the planet (approximately ecliptic longitude). The duration of the occultation determines the relative position of the planet and the compact radio source perpendicular to the direction of motion (i.e., approximately ecliptic latitude). One occultation can provide only two of the three parameters (Euler angles) needed for a full instantaneous frame-tie. However, one of the three parameters may be known well a priori, allowing a solution for the other two. Alternatively, a set of three orthogonal linear combinations of the three Euler angles can be found such that the occultation measurement has no sensitivity to one of the combinations. The other two can then be measured.

A. Frame-Tie Accuracy From Occultations

The accuracy of a planetary position measurement from an occultation event depends on several factors. Those that determine the measurement noise are

(1) the angular speed of the planet on the sky at the time of the event, ω,

(2) the strength of the radio source, S,

(3) the sensitivity (gain/system temperature) of the antenna used for the measurement, G/T_{sys}, and

(4) the geometry of the occultation.

The signal-to-noise ratio (S/N) for a single-dish total power measurement is [9]

$$S/N = \frac{SG\sqrt{BW\tau}}{KT_{sys}} \tag{1}$$

where S is the source flux density, G is the antenna gain, BW is the detected bandwidth, τ is the integration time, K is a dimensionless constant that depends on the detection system (it is 2 for a Dicke-switch system [9]), and T_{sys} is the system temperature. (Note that T_{sys} will have contributions from both the planet and the compact radio source.)

The integration time τ_{det} needed to detect the source is

$$\tau_{det} = \left(\frac{K\,(S/N)_{det}\,T_{sys}}{SG}\right)^2 \cdot \frac{1}{BW} \tag{2}$$

where $(S/N)_{det}$ is the S/N required to detect the source. This is a function of the detection system, but will probably be in the range 3–5. In the approximation of a very rapid change in received source power during ingress and egress (true for a compact source, an airless planet, and an occultation light curve governed by geometrical optics), the error in a position measurement is $\omega\tau_{det}$. This is the angular distance that the planet moves across the sky during the minimum integration time needed to detect the source (and, therefore, to detect its disappearance or reappearance). Because both ingress and egress times are needed, the errors in the planet–radio source positions are

$$\Delta\lambda = \sqrt{2}\omega\tau_{det} \tag{3}$$

$$\Delta\beta = \sqrt{2}\omega\tau_{det} \cdot \frac{1}{(dl/d\beta)} = \frac{\sqrt{2}\omega\tau_{det}\sqrt{y^2-1}}{2} \tag{4}$$

where λ and β are, respectively, the ecliptic longitude and latitude of the planet, $\Delta\lambda$ and $\Delta\beta$ are the errors in the measurement of these quantities, l is the arclength of the occultation chord on the disk of the planet, and y is the ratio of the angular radius of the planetary disk to the angular distance separating the occultation cord from the center of the disk ($y = r_p/z$ in Fig. 1). The term $dl/d\beta$ represents the dependence of the duration of the occultation (a measured quantity) on the difference between the ecliptic latitude of the planet and that of the radio source.

Equations (3) and (4) provide a lower limit to the frame-tie measurement error (an upper limit to the accuracy) from occultations. The finite observing frequency used for occultation measurements causes strong deviations from geometrical optics, resulting in a protracted Fresnel light curve lasting for several minutes of time instead of a sharp power change at ingress and egress. It has been shown [10] that the Fresnel pattern preserves all the Fourier components of a geometrical occultation pattern up to a limit set by the observing bandwidth. For a given occultation, there is an optimal bandwidth which will be a function of the telescope sensitivity and the observing frequency. For smaller bandwidths, the accuracy will degrade due to loss of S/N; for larger bandwidths, the accuracy will degrade due to loss of high-frequency Fourier components in the light curve. Therefore, the assumption of specific observing parameters (as in Section III) gives an accuracy estimate that is too optimistic if the actual bandwidth exceeds the optimal value. The atmosphere of a planet perturbs the Fresnel pattern (especially for Venus and Jupiter), and this perturbation introduces an additional source of error. Finally, fluctuations in receiver gain or in the terrestrial atmospheric contribution to the system temperature increase the measurement noise beyond that due solely to S/N limitations. Because of these three effects, which have not yet been studied in detail, Eqs. (3) and (4) can be used only to identify those occultation events that have the potential of an accurate frame-tie measurement.

B. Estimating Parameters of Candidate Events

The number and strength of radio sources that are occulted by a given planet depend on the area of sky that the planet sweeps out per unit time. This areal rate depends upon the angular size of the planet (Table 1) and its angular speed.

The average area of sky swept out by each planet per unit time is listed in Table 2. This average was computed for the 30-year period 1970–2000. There are two entries for each planet. The first is the area as viewed from the center of Earth (i.e., it does not take into account the nonzero size of Earth). The second column corrects this value for the parallax induced by the nonzero size of Earth (i.e., it includes the area on the sky that is occupied by part

of the planet as seen from at least some location on the surface of Earth). The apparent position of a planet with respect to objects outside the solar system differs from the geocentric position by an angle $R_\oplus \cos(el)/d_{pl}$, where $R_\oplus$ is Earth radius, el is the elevation of the planet above the horizon at the viewing location on Earth, and d_{pl} is the Earth–planet distance. This parallax can be as large as 40 arcsec for Venus at inferior conjunction. In contrast, it is always less than 3 arcsec for Jupiter.

For a given length of time, Venus occults many more sources of a given strength than Uranus or Neptune. Alternatively, in a given length of time, the brightest source occulted by Venus is almost always much stronger than the brightest source occulted by Uranus or Neptune. To quantify this, it is necessary to know the number density of compact radio sources on the sky as a function of source strength. Although the number density of the total flux density of radio sources is fairly well known [11], that of compact sources (requiring VLBI observations of each source) has been poorly studied. There has been only one survey covering the entire sky and a large number of sources. That survey [12] used intercontinental baselines and an observing frequency of 2.3 GHz. The survey revealed 227 sources with correlated flux density greater than 0.5 Jy. Some sources with correlated flux density greater than 0.5 Jy were missed due to the selection criteria used to determine which sources to observe (specifically, the lower limit for the total flux density was as large as 1 Jy in some parts of the sky). Therefore, the true number of sources with correlated flux densities greater than 0.5 Jy is perhaps around 300, or 0.0073 per square degree. A second correction is necessary. The fringe spacing of this survey was approximately 3 milliarcseconds (mas). Sources with sizes of 1–10 mas (compact enough to be useful for occultations) were partly resolved with this fringe spacing, so that the flux density usable for occultation measurements was underestimated. An approximate correction for this effect is to double the number density, giving 0.015 sources per square degree with compact flux density greater than 0.5 Jy. Within the 1–10-GHz range, this number density is probably only weakly dependent on observing frequency, so that the results from the 2.3-GHz survey can be used at other frequencies. The dependence on flux density is approximately $S^{-1.5}$, which is the value for a Euclidean universe with no source evolution. Thus

$$N(S > S_0) \approx 0.015 \left(\frac{S_0}{500 \text{ mJy}}\right)^{-1.5} \Omega_{deg}$$

$$= \left(\frac{S_0}{31 \text{ mJy}}\right)^{-1.5} \Omega_{deg}$$

where $N(S > S_0)$ is the number of radio sources with compact flux density greater than S_0 in a solid angle Ω_{deg} square degrees. Setting $N(S > S_0) = 1$ implies that there will be, on average, one source with compact flux density greater than $S_{threshold} = 31$ mJy $\Omega_{deg}^{2/3}$. The expected value $E(S_{max})$ for the brightest compact source in Ω_{deg} cannot be calculated without knowledge of the spatial correlation between sources. However, the expected total compact flux density in Ω_{deg} from sources stronger than $S_{threshold}$ is 3 $S_{threshold}$. If every patch of sky with solid angle Ω_{deg} had exactly one source with $S > S_{threshold}$, then

$$E(S_{max}) = 93 \text{ mJy } \Omega_{deg}^{2/3} \quad (5)$$

Because Eq. (5), which is used in this article, assumes a particular spatial correlation of sources, the true value of $E(S_{max})$ is somewhat different. Equation (5) and the values in the second column of Table 3 give the strength of the expected brightest compact radio source to be occulted by each planet in a given time interval. These flux densities are given in Table 3.

III. Searches for Planetary Occultations

Several radio-source catalogs have been searched for possible planetary occultations. This process involves several steps. The first step is to calculate the position of each planet during the time interval of the search, and compare this position to that of the radio sources in the catalog being searched. If a radio source lies within the angular distance $r_{pl} + p_{pl}$ from the path of the center of the planet (r_{pl} is the apparent angular radius of the planet and p_{pl} is the parallax induced for that planet at the limb of Earth), then an occultation occurs for at least some portion of the surface of Earth. The calculation requires that the combined position error for the planet and the radio source be at least as small as $r_{pl} + p_{pl}$, and preferably several times smaller. This constraint on the planetary position error is satisfied by all planets except Pluto. For radio sources, the magnitude of the position error depends strongly upon the individual catalog. Some catalogs are based upon VLBI or VLA observations and have position errors substantially less than 1 arcsec. However, catalogs based on searches with single radio antennas (these contain the majority of known radio sources) have position errors on the order of 1 arcmin. For searches performed with these catalogs, all that can be determined is whether or not a planet passes through the radio source position-error box. Further observations to improve the position knowledge of these occultation candidate sources are needed before it can be determined whether or not an occultation will occur.

The second step is to determine that portion of the Earth's surface for which the occultation will occur, and for which the planet and the radio source will be sufficiently far above the horizon to be observable with a radio telescope (typically about 10 deg). The position of the occultation chord on the planet varies over the region of the Earth's surface. Therefore, some sites will be more favorable than others for an accurate determination of the relative ecliptic latitude of the planet and radio source. The third step involves determining which radio telescopes, if any, are in that region.

Four catalogs of radio sources have been searched for planetary occultations. The results presented here are for the period July 1, 1990 to January 1, 2000, except for one event in 1988 which was observed.

The first catalog is the JPL Astrometric Catalog [3]. This catalog consists of strong, compact radio sources. Their correlated flux densities on intercontinental baselines are greater than about 300 mJy at both 2.3 and 8.4 GHz, and their positions have been determined to an accuracy of 5–10 nrad from extensive VLBI observations. They are all excellent sources for frame-tie measurements by planetary occultations. However, the version of the catalog used for the search has only 140 sources, which are distributed over the entire sky north of declination −45 deg. There is only one occultation event from this catalog, listed in Table 4.

The second catalog used for the search is a catalog of sources within 10 deg of the ecliptic. These sources all have correlated flux densities on intercontinental baselines greater than 100 mJy at 2.3 GHz [13] and are therefore all suitable for occultation measurements. The correlated flux densities of many of them have been measured at 8.4 GHz [14]. Their positions are known to an accuracy of about 0.3 arcsec [15–18]. The 144 sources in this catalog yielded two occultation events, listed in Table 4.

The third catalog is the VLA Calibrator Catalog. This consists of 679 sources with declinations greater than −50 deg. The positions of all these sources are known to an accuracy of better than 1 arcsec. The sources have been observed with the VLA at angular resolutions of 1 arcsec or better (0.1 arcsec for some sources) and have correlated flux densities greater than 200 mJy at that resolution for at least some centimeter wavelengths. However, their structures on smaller scales is in general not known. The source positions are known sufficiently well to determine which sources will be occulted, but VLBI observations are required to determine whether these sources are suitable for frame-tie measurements, and to obtain accurate (5–10 nrad) positions. One occultation event (see Table 4) was found for this catalog.

These three catalogs yielded four occultation events: three by Venus and one by Mercury. In order to find more events, a larger catalog that includes weaker, and therefore less well-studied sources, is needed. The Massachusetts Institute of Technology (MIT)–Green Bank Catalog [19] meets these requirements. It consists of approximately 6000 sources in the declination band (0°,+20°) and is mostly complete for 5-GHz flux densities above 100 mJy, as measured with the 2-arcmin beam of the Green Bank 91-m antenna. Position errors (3σ) are 90 arcsec. The area of sky covered by this catalog includes approximately 30 percent of the ecliptic. A search using the MIT–Green Bank Catalog yielded 212 candidate events (79 for Mercury, 72 for Venus, 50 for Mars, 8 for Jupiter, and 3 for Saturn), comprising 151 sources. A candidate event is defined as one in which at least part of a planetary disk passes within the 3σ position-error box of a radio source in the catalog.

For most of these candidate events, improved knowledge of the source position shows that no occultation occurs. For some events where an occultation does occur, the source is not sufficiently compact for a useful frame-tie measurement. VLA observations of the candidate sources can eliminate many of the unusable candidate events. With a position accuracy of about 0.3 arcsec, it is possible to determine which sources will actually be occulted, and with an angular resolution of 0.3–2 arcsec (depending on the observing frequency and the VLA configuration), it is possible to eliminate many sources that are too large for useful occultation measurements.

VLA observations have been made of sources for 164 of these 212 candidate events, including 112 of the 123 events occurring before 1995. Of these totals, VLA maps of 22 sources for 31 events [20] and of 9 sources for 13 events[1] have been made by others. VLA maps of 15 sources for 20 events were made for a different purpose [21]. Finally, VLA maps of 60 sources for 100 events were made in March 1988 specifically for the purpose of improving knowledge of candidate sources.

All known occultation events from the MIT–Green Bank Catalog are listed in Table 5. The flux densities in Table 5 are not those from the MIT–Green Bank survey, but from VLA measurements, which have a much smaller observing beam. Therefore, the flux densities are those

[1] G. Langston, personal communication, National Radio Astronomy Observatory, Charlottesville, Virginia.

of the compact components of the sources. Table 5 also includes one event from a VLA galactic plane survey.[2]

Some of the events in Table 5 can be easily eliminated as being incapable of yielding a frame-tie measurement. Some of them involve sources that are several arcseconds in extent (based on VLA observations) and therefore unsuitable for VLBI astrometry. The sources for four events (numbers 3, 8, 11, and 15) fall into this category. Other sources are too weak: $\omega\tau_{det}$, Eq. (2), is substantially larger than the current frame-tie error, even for a very sensitive receiving system (e.g., a DSN 70-m antenna with a maser receiver). Five events (numbers 4, 6, 9, 12, and 14) fall into this category. Furthermore, an analysis of the second event[3] listed in Table 5 has shown that a useful frame-tie measurement is not possible with the radio telescopes in the occultation path. That leaves five events from Table 5 that are potentially useful for frame-tie measurements.

Table 6 lists these five events plus the four events from Table 4, and gives information on the occultation regions on Earth and on the angular speed of the planet across the sky at the time of the occultation. Also included is the quantity $\omega\tau_{det}$ (the angular distance that the planet moves during a detection time) for a DSN 70-m antenna at 8.4 GHz (T_{sys} = 25 K off source, BW = 100 MHz) with $(S/N)_{det}$ = 5 and K = 2, see Eq. (2). The total 8.4-GHz flux density of the occulted source has been used, and contributions to the system temperature from the source and the planet have been included. The occultation paths for three of these events do not include a DSN site; the values in the sixth column of Table 6 are too optimistic in these cases.

Events 1 and 3–8 in Table 6 have the most potential of yielding useful frame-ties. The sources in events 2, 4, 5, 7, and 9 have not been observed with VLBI, so the size of the source (or, alternatively, the strength of any compact component) is not known. VLBI observations are necessary before the potential accuracy of a frame-tie measurement can be estimated. The last column in Table 6 gives a qualitative estimate of the probability of obtaining a useful frame-tie measurement from that event. This probability is based on the value of $\omega\tau_{det}$ for each event, and on the sizes of the radio telescopes that currently lie within the occultation region or are expected to lie within that region at the time of the event.

[2] J. S. Ulvestad, personal communication, Navigation Systems Section, Jet Propulsion Laboratory, Pasadena, California.

[3] R. P. Linfield, "The Next Two Known Planetary Occultation Events," JPL Interoffice Memorandum (internal document), Jet Propulsion Laboratory, Pasadena, California, April 4, 1989.

One additional catalog has been searched. The Parkes survey [22] covers the entire sky south of declination +4 deg at 2.3 GHz for sources brighter than 200 mJy. Seventy-eight candidate events (excluding those sources that are also in other catalogs) were found: 25 for Mercury, 33 for Venus, 16 for Mars, and 4 for Jupiter. Improved positions and angular sizes for the sources in these events are not yet available.

IV. Occultation Measurements

There are at least two methods of taking data during a planetary occultation. The first method is also the simplest—measuring the total system power at a single antenna as a function of time. The total system power consists of the off-source (e.g., cold sky) system temperature, antenna temperature from the planet, and antenna temperature from the compact radio source. In all cases of interest, the planet and the compact radio source fit into one primary antenna beam. Rapid time sampling (as fast as 50 msec for some events) is needed. The variations in received power must be sampled on a timescale comparable to the time it takes for the planet to move across the sky by the desired angular accuracy of the frame-tie. The total flux densities from the planets vary slowly with time, except for Jupiter at frequencies below about 100 MHz. Therefore, variations in antenna temperature are due to variations in received flux density from the source and to antenna tracking errors (i.e., time-dependent pointing errors). The latter are important in cases where the planet flux density is much greater than the source flux density. In these cases, variations in antenna temperature due to even minor tracking errors can be as large as or larger than variations due to the occultation process.

Table 7 lists approximate planet flux densities at three frequencies for the nine events in Table 6. These values are derived from the angular sizes of the planets at the occultation epochs and the average measured brightness temperatures [23]. It can be seen that the flux densities of planets, which are due to thermal emission in the Rayleigh-Jeans tail of a black-body distribution, are much lower at 2.3 GHz than at 8.4 or 22 GHz. Therefore, the contrast between a flat-spectrum radio source, with a flux density that is approximately independent of observing frequency, and a planet is greatest at low frequencies. Furthermore, primary antenna beams are larger at low frequencies, making the variations in total power due to antenna tracking errors much less important as the frequency decreases. Two effects cause the accuracy to improve as the observing frequency increases: the effects of the planet's ionosphere decrease and the deviation of the light curve from that due to

geometrical optics decreases, due to a shorter wavelength. The value of the optimum observing frequency has not yet been determined, but it is certainly different for different events.

A second, alternative method of taking data during a planetary occultation consists of making VLBI measurements with two radio telescopes on the compact radio source during the occultation. Consider the case where only one of the two telescopes is in the occultation region. The variation in correlated flux density in this case follows the square root of the variation in antenna temperature at the telescope where the occultation occurs. This method has two potential advantages over the first method. The first advantage is stability. Interferometric measurements are much less sensitive to receiver gain variations (which affect the output voltage but not the system temperature) than are single-dish measurements. Also, interferometric observations are insensitive to variations in the antenna temperature of the planet (due to tracking errors) to first order, because the planetary emission is completely resolved and does not contribute to the correlated flux density. (A second-order effect occurs because tracking errors cause small fractional variations in the total system temperature, which then cause correspondingly small fractional variations in the correlated flux density). There is a second advantage when the telescope in the occultation region is much less sensitive than the one outside. The sensitivity of a two-element interferometer is proportional to the geometric mean of the sensitivities of its two antennas. If both telescopes are in the occultation region, the first advantage still holds; however, the interpretation of correlated flux density variations will be more complicated.

The main drawback of the second method is a loss in sensitivity compared to single-dish measurements. One-bit clipping in current VLBI systems causes a loss of a factor of $\frac{\pi}{2} = 1.57$ compared to single-dish observations. Details of VLBI correlators (e.g., a finite number of levels in the lobe rotator) increase this factor to about 2.5. In addition, the bandwidth available for VLBI recording (56 MHz with the Mk III system or 112 MHz for Mk III recorders equipped with 4-MHz filters) is often less than the bandwidth available for single-dish observations.

The first event in Table 6 occurred in July 1988, when Venus occulted the radio source 0507+17. Total-power measurements were taken during this occultation with the DSS 43 70-m antenna at a frequency of 2.3 GHz. The sampling time was 50 msec. Both ingress and egress were clearly seen, and analysis of the data is now in progress. Observing plans for future events will be made as more information about the sources involved is gathered and the epoch of each event approaches.

Acknowledgments

The author thanks R. N. Treuhaft and X X Newhall for useful comments on early drafts of this manuscript. E. M. Standish and X X Newhall provided software that was useful in the calculation of occultation events.

References

[1] J. S. Border, F. F. Donivan, S. G. Finley, C. E. Hildebrand, B. Moultrie, and L. J. Skjerve, "Determining Spacecraft Angular Position with Delta VLBI: The Voyager Demonstration," AIAA Paper 82-1471, presented at the 1982 AIAA Conference, San Diego, California, August 1982.

[2] R. N. Treuhaft, "Deep Space Tracking in Local Reference Frames," *TDA Progress Report 42-94*, vol. April–June 1988, Jet Propulsion Laboratory, Pasadena, California, pp. 1–15, August 15, 1988.

[3] O. J. Sovers, C. D. Edwards, C. S. Jacobs, G. E. Lanyi, K. M. Liewer, and R. N. Treuhaft, "Astrometric Results of 1978–1985 Deep Space Network Radio Interferometry: The JPL 1987-1 Extragalactic Source Catalog," *Astronomical Journal*, vol. 95, no. 6, pp. 1647–1658, 1988.

[4] R. W. Porcas, "Summary of Known Superluminal Sources," in *Superluminal Radio Sources*, J. A. Zensus and T. J. Pearson, eds., Cambridge: Cambridge University Press, 1987.

[5] E. M. Standish, "Celestial Reference Frames: Definitions and Accuracies," in *The Impact of VLBI on Astrophysics and Geophysics*, IAU Symposium no. 129, M. J. Reid and J. M. Moran, eds., Boston: Kluwer Academic Publishers, 1988.

[6] A. E. Niell, X X Newhall, R. A. Preston, G. L. Berge, D. O. Muhleman, D. J. Rudy, J. K. Campbell, P. B. Esposito, and E. M. Standish, "Relating the Planetary Ephemerides and the Radio Reference Frame," *TDA Progress Report 42-81*, vol. January–March 1985, Jet Propulsion Laboratory, Pasadena, California, pp. 1–8, May 15, 1985.

[7] J. G. Williams, "Determining Asteroid Masses From Perturbations on Mars," *Icarus*, vol. 57, no. 1, pp. 1–13, 1984.

[8] W. M. Folkner, "Navigational Utility of High-Precision Radio Interferometry for Galileo's Approach to Jupiter," *TDA Progress Report 42-102*, vol. July–September 1990, Jet Propulsion Laboratory, Pasadena, California, pp. 34–46, November 15, 1990.

[9] A. R. Thompson, J. M. Moran, and G. W. Swenson, Jr., *Interferometry and Synthesis in Radio Astronomy*, New York: John Wiley & Sons, 1986.

[10] P. A. G. Scheuer, "On the Use of Lunar Occultations for Investigating the Angular Structure of Radio Sources," *Australian Journal of Physics*, vol. 15, no. 2, pp. 332–343, 1962.

[11] J. V. Wall and J. A. Peacock, "Bright Extragalactic Radio Sources at 2.7 GHz — III. The All-Sky Catalog," *Monthly Notices of the Royal Astronomical Society*, vol. 216, no. 1, pp. 173–192, 1985.

[12] R. A. Preston, D. D. Morabito, J. G. Williams, J. Faulkner, D. L. Jauncey, and G. D. Nicolson, "A VLBI Survey at 2.29 GHz," *The Astronomical Journal*, vol. 90, no. 9, pp. 1599–1641, 1985.

[13] A. E. Wehrle, D. D. Morabito, and R. A. Preston, "Very Long Baseline Interferometry Observations of 257 Extragalactic Radio Sources in the Ecliptic Region," *Astronomical Journal*, vol. 89, no. 3, pp. 336–341, 1984.

[14] D. D. Morabito, A. E. Niell, R. A. Preston, R. P. Linfield, A. E. Wehrle, and J. Faulkner, "VLBI Observations of 416 Extragalactic Radio Sources," *Astronomical Journal*, vol. 91, no. 5, pp. 1038–1050, 1986.

[15] D. D. Morabito, R. A. Preston, M. A. Slade, and D. L. Jauncey, "Arcsecond Positions for Milliarcsecond VLBI Nuclei of Extragalactic Radio Sources: I. 546 Sources," *Astronomical Journal*, vol. 87, no. 3, pp. 517–527, 1982.

[16] D. D. Morabito, R. A. Preston, M. A. Slade, D. L. Jauncey, and G. D. Nicolson, "Arcsecond Positions for Milliarcsecond VLBI Nuclei of Extragalactic Radio Sources: II. 207 Sources," *Astronomical Journal*, vol. 88, no. 8, pp. 1138–1145, 1983.

[17] D. D. Morabito, A. E. Wehrle, R. A. Preston, R. P. Linfield, M. A. Slade, J. Faulkner, and D. L. Jauncey, "Arcsecond Positions for Milliarcsecond VLBI Nuclei of Extragalactic Radio Sources: III. 74 Sources," *Astronomical Journal*, vol. 90, no. 4, pp. 590–594, 1985.

[18] D. D. Morabito, R. A. Preston, R. P. Linfield, M. A. Slade, and D. L. Jauncey, "Arcsecond Positions for Milliarcsecond VLBI Nuclei of Extragalactic Radio Sources: IV. Seventeen Sources," *Astronomical Journal*, vol. 92, no. 3, pp. 546–551, 1986.

[19] C. L. Bennett, C. R. Lawrence, B. F. Burke, J. N. Hewitt, and J. Mahoney, "The MIT–Green Bank 5 GHz Survey," *Astrophysical Journal Supplement*, vol. 61, no. 1, pp. 1–104, 1986.

[20] C. R. Lawrence, C. L. Bennett, J. N. Hewitt, G. I. Langston, S. E. Klotz, and B. F. Burke, "5 GHz Radio Structure and Optical Identifications of Sources from the MG Survey: II. Maps and Finding Charts," *Astrophysical Journal Supplement*, vol. 61, no. 1, pp. 105–157, 1986.

[21] R. P. Linfield and J. S. Ulvestad, "Source and Event Selection for Radio-Planetary Frame-Tie Measurements Using the Phobos Lander," *TDA Progress Report 42-92*, vol. October–December 1987, Jet Propulsion Laboratory, Pasadena, California, pp. 1–12, February 15, 1988.

[22] J. G. Bolton, A. E. Wright, and A. Savage, "The Parkes 2700 MHz Survey: XIV. Catalogue for Declinations $-4°$ to $-15°$, Right Ascensions 10^h to 15^h," *Australian Journal of Physics Astrophysics Supplement*, no. 46, 1979.

[23] J. D. Kraus, *Radio Astronomy*, Powell, Ohio: Cygnus-Quasar Books, 1986.

Table 1. Angular sizes of the planets

Planet	Range of apparent angular radius, arcsec
Mercury	2 – 6
Venus	5 – 30
Mars	2 – 12
Jupiter	15 – 25
Saturn	7 – 10
Uranus	1.6 – 1.9
Neptune	1.0 – 1.4
Pluto	0.06 – 0.1

Table 2. Solid angle of sky swept up by planets

Planet	Solid angle viewed from center of Earth, square deg/yr	Solid angle from anywhere on Earth, square deg/yr
Mercury	0.78	2.8
Venus	1.7	3.5
Mars	0.34	0.96
Jupiter	0.49	0.53
Saturn	0.12	0.13
Uranus	0.012	0.016
Neptune	0.0047	0.0059
Pluto	0.0005	0.002

Table 3. Expected brightest compact radio sources to be occulted

Planet	Expected brightest source, mJy $t_{yr}^{0.67}$
Mercury	185
Venus	215
Mars	90
Jupiter	61
Saturn	24
Uranus	6
Neptune	3
Pluto	1

Table 4. Occultation events from VLBI and VLA catalogs

Event	Date	Planet	Radio source	Catalog	Correlated flux density on long baselines, Jy	
					2.3 GHz	8.4 GHz
1	July 19, 1988	Venus	0507+17	DSN	0.3	0.6
2	Nov. 11, 1992	Venus	1748−253	VLA	—	0.5[a]
3	Mar. 7, 1996	Mercury	2208−137	Ecliptic	0.2	< 0.07
4	Mar. 6, 1998	Venus	2008−159	Ecliptic	0.4	0.4

[a] This is the correlated flux density on a 35-km baseline at 5 GHz. The correlated flux density on longer baselines is not known.

Table 5. Occultation events from the MIT-Green Bank Catalog and the Galactic Plane Survey

Event	Date	Planet	Radio source	Peak flux density, mJy	VLA observation frequency, GHz	Angular resolution, arcsec
1	Oct. 5, 1991	Jupiter	MG1027+1033	26	8.4	2
2	Jan. 15, 1992	Mercury	1831−237E	80	5.0	0.3[a]
3	July 18, 1992	Jupiter	MG1058+0748[b]	11	8.4	2
4	Aug. 23, 1992	Mercury	MG0900+1654[b]	18	8.4	2
5	Oct. 7, 1992	Jupiter	MG1159+0111	94	8.4	2[c]
6	May 6, 1993	Mercury	MG0211+1143	14	8.4	2
7	June 18, 1993	Venus	MG0242+1248	103	5.0	0.3
8	April 15, 1995	Mercury	MG0137+0929[b]	79	5.0	1
9	June 27, 1995	Mars	MG1112+0559[b]	15	8.4	2
10	Oct. 1, 1996	Mars	MG0905+1755	65	8.4	2
11	July 15, 1997	Mercury	MG0900+1831[b]	29	5.0	0.3
12	July 19, 1997	Venus	MG0949+1449	7	8.4	2
13	Aug. 30, 1998	Mercury	MG0925+1444	41	8.4	2
14	July 6, 1999	Venus	MG0954+1244	5	8.4	2
15	Aug. 19, 1999	Mercury	MG0843+1813[b]	16	5.0	0.3

[a] Multifrequency observations show that this source has a flat spectrum.

[b] This source has multiple components, at least two of which will be occulted. The flux density of the brightest occulted component is listed.

[c] VLBI observations at 8.4 GHz with 0.02″ resolution show correlated flux density of 75 mJy.

Table 6. Details on apparently useful occultation events

Event	Date	Planet	Angular velocity on the sky, arcsec/min	Occultation region on Earth	$\omega\tau_{det}$ for 8.4-GHz DSN 70-m system, nrad	Probability of useful frame-tie
1	July 19, 1988	Venus	1.21	Australia	0.6	High
2	Oct. 5, 1991	Jupiter	0.49	Europe, Asia, Africa, western Australia	80	Low
3	Oct. 7, 1992	Jupiter	0.53	North America (except west coast), Europe, Africa, South America	7	Moderately High
4	Nov. 11, 1992	Venus	3.01	South America	1	Medium
5	June 18, 1993	Venus	2.52	North America, eastern Australia	35	Medium
6	Mar. 7, 1996	Mercury	4.04	South America, southern Africa	1	Medium
7	Oct. 1, 1996	Mars	1.50	Australia	30	Medium
8	Mar. 6, 1998	Venus	1.95	Antarctica	0.5	Medium
9	Aug. 30, 1998	Mercury	2.30	North America, England, Spain	100	Low

Table 7. Flux densities of the planets during occultation events

Event	Date	Planet	Planet flux density at 2.3 GHz, Jy	Planet flux density at 8.4 GHz, Jy	Planet flux density at 22 GHz, Jy
1	July 19, 1988	Venus	2.4	30	200
2	Oct. 5, 1991	Jupiter	0.8	6	35
3	Oct. 7, 1992	Jupiter	0.8	6	30
4	Nov. 11, 1992	Venus	0.4	5	30
5	June 18, 1993	Venus	0.8	10	80
6	Mar. 7, 1996	Mercury	0.03	0.4	3
7	Oct. 1, 1996	Mars	0.013	0.2	1.2
8	Mar. 6, 1998	Venus	1.8	20	170
9	Aug. 30, 1998	Mercury	0.06	0.8	6

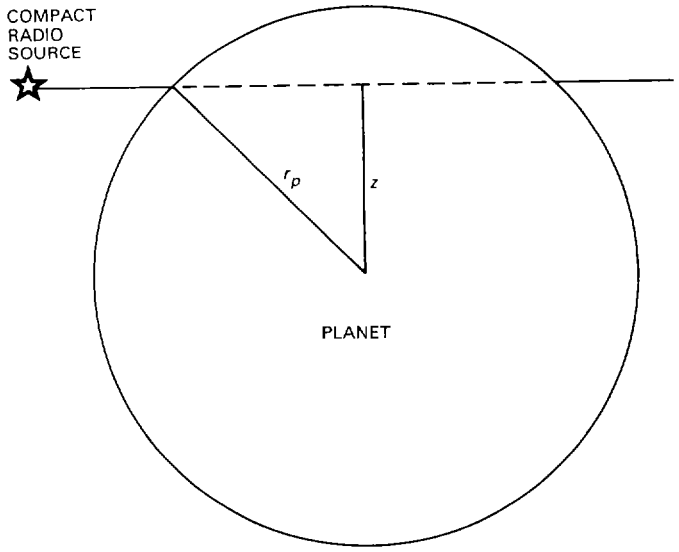

Fig. 1. Geometry of a planetary occultation.